Effect of hyperon bulk viscosity on neutron-star *r*-modes

Lee Lindblom
Theoretical Astrophysics 130-33, California Institute of Technology, Pasadena, California 91125

Benjamin J. Owen
Department of Physics, University of Wisconsin–Milwaukee, P.O. Box 413, Milwaukee, Wisconsin 53201
and Albert Einstein Institut (Max Planck Institut für Gravitationsphysik), Am Mühlenberg 1, 14476 Golm, Germany
(Received 25 October 2001; published 4 March 2002)

Neutron stars are expected to contain a significant number of hyperons in addition to protons and neutrons in the highest density portions of their cores. Following the work of Jones, we calculate the coefficient of bulk viscosity due to nonleptonic weak interactions involving hyperons in neutron-star cores, including new relativistic and superfluid effects. We evaluate the influence of this new bulk viscosity on the gravitational radiation driven instability in the *r*-modes. We find that the instability is completely suppressed in stars with cores cooler than a few times 10^9 K, but that stars rotating more rapidly than 10–30% of maximum are unstable for temperatures around 10^{10} K. Since neutron-star cores are expected to cool to a few times 10^9 K within seconds (much shorter than the *r*-mode instability growth time) due to direct Urca processes, we conclude that the gravitational radiation instability will be suppressed in young neutron stars before it can significantly change the angular momentum of the star.

DOI: 10.1103/PhysRevD.65.063006 PACS number(s): 97.60.Jd, 04.30.Db, 04.40.Dg, 26.60.+c

I. INTRODUCTION

The *r*-modes (fluid oscillations whose dynamics is dominated by rotation) of neutron stars have received considerable attention in the past few years because they appear to be subject to the Chandrasekhar-Friedman-Schutz gravitational radiation instability in realistic astrophysical conditions (see Ref. [1] for a recent review). If the *r*-modes are unstable, i.e. if the damping time scales due to viscous processes in neutron-star matter are longer than the gravitational-radiation driving time scale, a rapidly rotating neutron star could emit a significant fraction of its rotational energy and angular momentum as gravitational waves. With appropriate data analysis strategies, these waves could be detectable by interferometers comparable to the enhanced Laser Interferometric Gravitational Wave Observatory (LIGO) interferometers. The *r*-mode instability might also explain the relatively long spin periods observed in young pulsars and of older, accreting pulsars in low-mass x-ray binaries.

Recently Jones [2,3] has pointed out that long-neglected processes involving hyperons (massive cousins of the nucleons) can lead to an extremely high coefficient of bulk viscosity in the core of a neutron star. Using simple scaling arguments he suggests that the viscous damping time scales associated with these processes may be short enough to suppress the *r*-mode instability altogether in realistic astrophysical circumstances. The purpose of this paper is to investigate this possibility more thoroughly. The hyperons only exist in the central core of a neutron star where the density is sufficiently high. The relevant effects of the *r*-modes however vanish as r^6 (where r is the distance from the center of the star). Thus the overall effect of hyperon induced dissipation on the *r*-modes depends very sensitively on the size and structure of the core of a neutron star. Jones' initial estimates did not take properly into account either the structure of the *r*-mode or the detailed properties of the nuclear matter in the core of a neutron star. We improve on Jones' analysis in several ways: First we evaluate fully relativistic cross sections to determine the reaction rates of the relevant hyperon interactions. We find that these cross sections reduce to the results of Jones [2,4] in the low-momentum limit, but can be about an order of magnitude larger in some regimes of neutron-star matter. Second we derive new expressions for the bulk viscosity coefficient that are appropriate even for a relativistic fluid such as neutron star matter. Third we construct detailed neutron star models based on an equation of state that includes hyperons and the appropriate interactions among all of the particle species present. Due to superfluid effects the temperature and density dependence of hyperon bulk viscosity turns out to be quite complicated: superfluidity increases the viscosity in some cases while reducing it in others. And fourth, we use a more accurate model of the structure of the *r*-mode eigenfunction in the cores of these stars to evaluate the effects of hyperon dissipation.

Our analysis shows that hyperon bulk viscosity completely suppresses the gravitational radiation instability in the *r*-modes of rotating neutron stars for temperatures below a few times 10^9 K. We find that the gravitational radiation instability acts most strongly at temperatures around 10^{10} K where stars rotating more than 10–30% of the maximum rotation rate (depending on the details of the microphysics) are driven unstable. Our coefficient of bulk viscosity is actually several hundred times that of Jones [2,3], who suggested that the instability was completely suppressed. However, our use of the proper *r*-mode eigenfunction reduces the dissipation by several orders of magnitude and we find that there is a window of instability. How long it lasts is another matter. If the core of the neutron star cools via the standard modified Urca process, its temperature remains above a few times 10^9 K for about a day [5]. This is enough time for an un-

stable *r*-mode to grow and radiate away a substantial fraction of the star's rotational kinetic energy and angular momentum into gravitational waves [6]. However if the core of the star cools too quickly the instability might not have enough time to grow before being suppressed by the hyperon bulk viscosity. The time needed for a neutron-star core to cool to a few times 10^9 K is reduced to about a second when direct Urca processes are able to act [7,8]. Modern equations of state have large enough proton densities in the core that direct Urca cooling is now expected to act until the neutrons and protons condense into a superfluid state, i.e., above about 10^9 K. The growth time for the gravitational radiation instability in the most rapidly rotating neutron stars is about 40 s [9]. Thus we conclude that the core of a neutron star will probably cool too quickly for the *r*-mode instability to grow significantly before being suppressed by the hyperon bulk viscosity.

The organization of the rest of this paper is as follows. In Sec. II we provide details of the equation of state which we use, including numerical aspects of the evaluation of various thermodynamic variables and derivatives, and the model of hyperon superfluidity that we employ. In Sec. III we present a new derivation of the coefficient of bulk viscosity for relativistic neutron-star matter (including several interacting fluids) in terms of the microscopic reaction rates and thermodynamic derivatives. In Sec. IV, we compute the relevant cross sections in order to evaluate the reaction rates for hyperons in a dense medium. In Sec. V we combine the thermodynamic expressions of Sec. III with the microscopic reaction rates of Sec. IV to obtain expressions for hyperon bulk viscosity as a function of density and temperature in neutron-star matter. In Sec. VI we evaluate *r*-mode damping time scales for neutron stars containing ordinary fluid and superfluid hyperons. Finally, in Sec. VII we discuss the implications of our results for the *r*-mode instability in real neutron stars, and we also attempt to estimate how robust these conclusions are.

II. EQUATION OF STATE

A. Thermodynamic equilibrium

Neutron-star matter is a Fermi liquid which at low densities is composed primarily of neutrons n, protons p and electrons e. Charge neutrality $n_p = n_e$ (where n_i is the number density of the ith species) and β-equilibrium $\mu_n = \mu_p + \mu_e$ (where μ_i is the chemical potential of the ith species) determine the relative concentrations of these particles at each density. As the total baryon density increases however, it becomes energetically favorable for the equilibrium state to include additional particle species: first muons μ, and then a sequence of hyperons Σ^-, Λ, ... These additional particles appear as the density exceeds the threshold for the creation of each new species. The relative concentrations of the various species are determined at each density by imposing charge neutrality and β-equilibrium. At the highest densities of interest to us these equilibrium constraints are

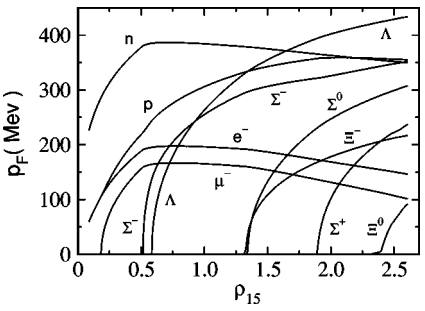

FIG. 1. Fermi momenta (in MeV) of the baryons and leptons as functions of total energy density (in 10^{15} g/cm^3) for Glendinning's equation of state.

$$n_p = n_e + n_\mu + n_{\Sigma^-}, \tag{2.1}$$

$$\mu_p = \mu_n - \mu_e, \tag{2.2}$$

$$\mu_\mu = \mu_e, \tag{2.3}$$

$$\mu_{\Sigma^-} = \mu_n + \mu_e, \tag{2.4}$$

$$\mu_\Lambda = \mu_n. \tag{2.5}$$

In order to solve these constraints and determine the equilibrium state of neutron-star matter, we need explicit expressions for the various chemical potentials μ_i as functions of the particle number densities n_j. These functions have encoded within them the details of the interactions between the various particles in a dense Fermi-liquid environment. In this paper we have adopted the expressions for these chemical potentials as given by Glendenning's relativistic effective mean-field theory [10,11]. Figure 1 illustrates the Fermi momenta of the various particle species as a function of the total energy density of the matter that we obtained with Glendenning's (case 2 [10]) expressions for the chemical potentials. Glendenning also gives expressions for the total energy density ρ and total pressure p as functions of the particle densities n_i. These quantities are illustrated and tabulated by Glendenning [10,11], and we will not reproduce them here. Our numerical code reproduces Glendenning's numbers quite accurately.

We are also interested here in some less familiar thermodynamic quantities that are relevant for calculating the bulk viscosity in neutron-star matter. These quantities are easily determined once the full description of the equilibrium state is known. In particular the partial derivatives of the chemical potentials with respect to the various particle number densities, $\alpha_{ij} \equiv \partial \mu_i / \partial n_j$, are needed in the expression for the relaxation time associated with bulk visocity as defined in Eqs. (3.16), (3.24), and (3.25) below. These α_{ij} are easily determined numerically (or even analytically in some cases) once the full equilibrium state is known. Further the thermodynamic function

$$\gamma_\infty - \gamma_0 \equiv -\frac{n_B^2}{p} \frac{\partial p}{\partial n_n} \frac{d\tilde{x}_n}{dn_B}, \tag{2.6}$$

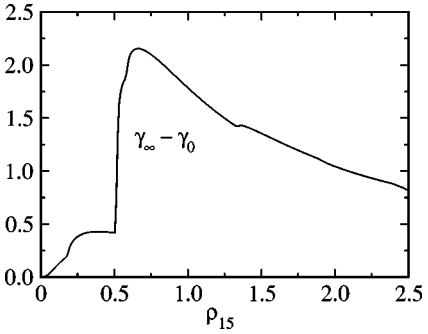

FIG. 2. Thermodynamic prefactor $\gamma_\infty - \gamma_0$ (the difference between the ''fast'' and ''slow'' adiabatic indices) that appears in our expression for the bulk viscosity.

appears as a prefactor in the expression for the bulk viscosity, Eq. (3.11), that we derive below. Here $\partial p/\partial n_n$ is just the partial derivative of the pressure with respect to the number density of neutrons (keeping the other number densities fixed), and $d\tilde{x}_n/dn_B$ is the derivative of the fractional density of neutrons in the equilibrium state, $\tilde{x}_n = n_n/n_B$, with respect to the total baryon density n_B. The left side of Eq. (2.6) has been re-expressed in terms of γ_∞ the ''fast'' and γ_0 the ''slow'' adiabatic indices defined in Eqs. (3.12) and (3.13) below. Figure 2 illustrates this function for the Glendenning equation of state. For a non-relativistic fluid the pre-factor $p(\gamma_\infty - \gamma_0)$ is identical to a commonly used alternative expression involving the sound speeds of the fluid: $\rho(u_\infty^2 - u_0^2)$ [12]. However, this equality is not satisfied in neutron-star matter. Consequently it is important to use the correct expression given in Eq. (2.6).

We have solved the relativistic structure equations for the non-rotating stellar models based on this equation of state. Figure 3 illustrates the total energy density as a function of radius for neutron-star models having a range of astrophysically relevant masses. This figure illustrates that these stars contain large central cores having material at densities that exceed the Σ^- and Λ threshold densities. The fact that it becomes energetically favorable to create hyperons (or even free quarks) above some threshold density is not really very controversial. However the expressions for the chemical potentials as functions of the particle densities are not well

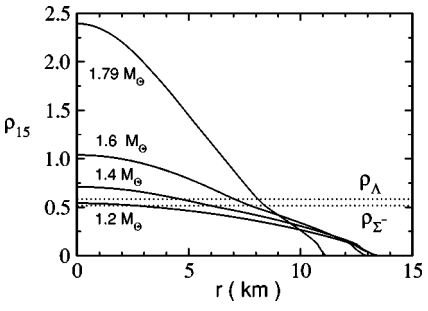

FIG. 3. Structure of neutron stars having a range of masses using Glendinning's equation of state: total energy density (in units of 10^{15} g/cm^3) vs distance from the center of the star. Threshold densities for Σ^- and Λ hyperon formation are also plotted. These equilibrium structures are computed using general relativity.

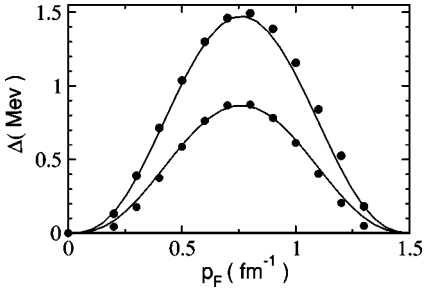

FIG. 4. Comparison of the zero-temperature superfluid gap function Δ_Λ as calculated by Balberg and Barnea (dots) with the empirical analytical fit in Eq. (2.7) (curves). The bottom and top curves correspond to $n_B = 0.4$ and 0.8 fm^{-3} respectively.

known, and so the detailed properties of nuclear matter at the densities where hyperons are likely to occur is not well determined at this time. This uncertainty translates then to an uncertainty about the sizes of the hyperon containing cores of real neutron stars. Since the size of this hyperon core determines the strength of the bulk viscosity effects which we evaluate here, the implications for the stability of the *r*-modes are correspondingly uncertain as well.

B. Superfluidity

Next, we must consider the possibility that the hyperons in neutron-star matter form Cooper pairs and condense into a superfluid state at sufficiently low temperatures. Various calculations are given in the literature of the Λ superfluid gap function Δ_Λ [13,14]. The Λ gap function is constrained by the experimental data on the energy levels of double Λ hypernuclei such as ${}^{10}_{\Lambda\Lambda}$Be and ${}^{13}_{\Lambda\Lambda}$B [14], however even so it is probably only known to within a factor of 2 or 3. In our numerical analysis of the bulk viscosity time scales discussed in Sec. V we use an analytical fit to the zero-temperature gap function Δ_Λ as computed by Balberg and Barnea [13]. Their calculation produces a gap that depends on the total baryon density n_B of the nuclear matter and on the Fermi momentum p_F of the Λ itself. As illustrated in Fig. 4 we find that the empirical fit

$$\Delta_\Lambda(p_F, n_B) = 5.1 p_F^3 (1.52 - p_F)^3 \times [0.77 + 0.043(6.2 n_B - 0.88)^2], \quad (2.7)$$

matches their calculated values for the zero-temperature gap energies fairly well. In this expression the gap energy is measured in MeV, p_F is measured in fm^{-1}, and n_B is measured in fm^{-3}.

The Σ^- superfluid gaps are not as well determined because comparable experimental data on double Σ^- hypernuclei do not exist at present. Calculations by Takatsuka *et al.* [14] using several models of the nuclear interaction give values of Δ_{Σ^-} in the range: $\Delta_\Lambda \lesssim \Delta_{\Sigma^-} \lesssim 10\Delta_\Lambda$. We perform two sets of calculations based on the extremes of this range. We either set $\Delta_{\Sigma^-} = \Delta_\Lambda$ or $\Delta_{\Sigma^-} = 10\Delta_\Lambda$. By equality here we mean that the dependence of Δ_{Σ^-} on n_B and p_F (up to the overall factor of 10) is given by Eq. (2.7). Using these energy gaps, and the Glendenning equation of state, we can evaluate

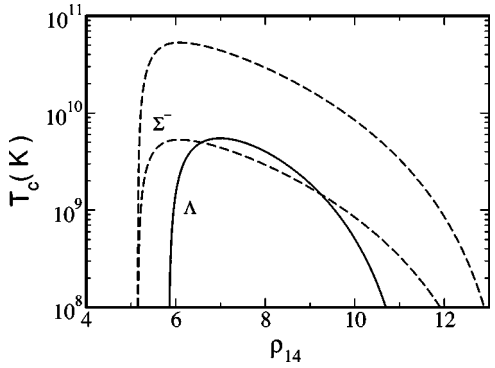

FIG. 5. Superfluid critical temperatures as functions of the total energy density (in units of 10^{14} g/cm^3). The solid curve is for Λ hyperons, while the dashed curves are for Σ^- hyperons using either $\Delta_{\Sigma^-}=\Delta_\Lambda$ (bottom) or $\Delta_{\Sigma^-}=10\Delta_\Lambda$ (top).

then the density dependence of the superfluid gap functions. We illustrate these in the form of superfluid critical temperatures T_c [which are related to the zero-temperature gap functions by $kT_c=0.57\Delta(0)$] in Fig. 5.

The superfluid gap depends not only on the density of the superfluid material, as discussed above, but also on its temperature. This temperature dependence will be needed to determine the temperature dependence of the hyperon bulk viscosity below. The standard BCS model calculation [15] of the temperature dependence of the gap is illustrated in Fig. 6. This figure compares the results of the exact calculation with a simple empirical fit to these data:

$$\Delta(T)=\Delta(0)\left[1-\left(\frac{T}{T_c}\right)^{3.4}\right]^{0.53}. \tag{2.8}$$

Since this fit is quite good, we use it whenever the temperature dependence of the gap is needed.

III. BULK VISCOSITY

Bulk viscosity is the dissipative process in which the macroscopic compression (or expansion) of a fluid element is converted to heat. The formalism for calculating the bulk viscosity coefficient in terms of the relaxation times of the microscopic processes which effect the conversion is well-known—see, e.g., Landau and Lifschitz [12]. However, such calculations are generally performed for an ordinary fluid like air, in which the microscopic processes (typically involving the transfer of energy between rotational and vibrational degrees of freedom of the molecules) can be taken to be independent. In neutron-star matter there are several relevant microscopic processes (involving weak interactions between the various particle species), but they are related by constraints (such as conservation of baryon number)—meaning that we cannot simply use the standard formulas for either a single process or multiple processes. Further, neutron-star matter is composed of some particles having relativistic energies. The standard expressions for bulk viscosity are not correct for such materials. In this section we present a modified and expanded derivation of the equations of bulk viscosity appropriate for neutron-star matter.

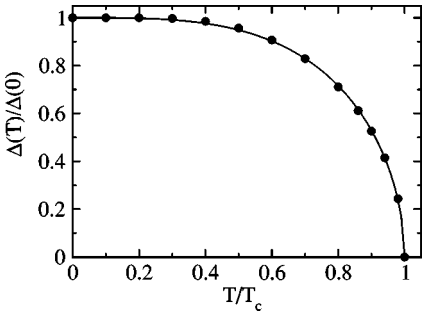

FIG. 6. Temperature dependence of the superfluid gap: exact values (points) compared to the empirical analytical fit (curve) given in Eq. (2.8). The critical temperature T_c is related to the zero-temperature gap energy by $kT_c=0.57\Delta(0)$.

Bulk viscosity is due to an instantaneous difference between the total physical pressure p of a fluid element and the thermodynamic pressure $\tilde{p}$. The thermodynamic pressure is determined only by the equation of state for a fluid element of given particle number and entropy densities. It is the value toward which the microscopic processes are driving the physical pressure at any given time. The coefficient of bulk viscosity ζ defines the proportionality of this pressure difference to the macroscopic expansion of the fluid:

$$p-\tilde{p}=-\zeta\vec{\nabla}\cdot\vec{v}, \tag{3.1}$$

where $\vec{v}$ is the velocity of the fluid element.

Consider now a fluid state that is an infinitesimal perturbation of a time-independent equilibrium state. Let p_0 and n_0 denote the pressure and number density (functions only of position) that describe this equilibrium state. To calculate ζ in terms of the microscopic reaction rates that drive the system toward equilibrium, we re-express both sides of Eq. (3.1) in terms of the Lagrangian perturbation of the particle number density $\Delta n\equiv n-n_0$. Using the particle conservation equation (and keeping only terms linear in the deviation away from equilibrium), we express the right side of Eq. (3.1) as

$$-\zeta\vec{\nabla}\cdot\delta\vec{v}=-i\hat{\omega}\zeta\Delta n/n, \tag{3.2}$$

where $\delta\vec{v}$ is the Eulerian velocity perturbation, and we assume that the perturbation has time dependence $e^{-i\hat{\omega}t}$ in the comoving frame of the fluid.

In order to analyze the left side of Eq. (3.1), we examine a fluid variable x that characterizes the microscopic process which produces bulk viscosity. For small departures from equilibrium, the value of x in the physical fluid state relaxes toward its value in thermodynamic equilibrium by

$$\partial_t x+\vec{v}\cdot\vec{\nabla}x=-(x-\tilde{x})/\tau, \tag{3.3}$$

where τ is defined as the relaxation time for this process. We are interested in nearly equilibrium fluid states in which the physical values of the state variable x (and hence the thermodynamic state $\tilde{x}$) oscillate about the background equilibrium, so that

$$(\partial_t+\vec{v}\cdot\vec{\nabla})(x-x_0)=-i\hat{\omega}(x-x_0), \tag{3.4}$$

$$(\partial_t+\vec{v}\cdot\vec{\nabla})(\tilde{x}-x_0)=-i\hat{\omega}(\tilde{x}-x_0). \tag{3.5}$$

In such a state it is straightforward to verify that

$$x-x_0=\frac{x-\tilde{x}}{i\hat{\omega}\tau}=\frac{\tilde{x}-x_0}{1-i\hat{\omega}\tau}. \tag{3.6}$$

Now consider how the fluid variable $\tilde{x}$ changes as the particle number density of the state is varied slowly from one equilibrium state to another:

$$\tilde{x}-x_0=\frac{d\tilde{x}}{dn}(\tilde{n}-n_0)=\frac{d\tilde{x}}{dn}\Delta n \tag{3.7}$$

(since by definition $\tilde{n}=n$). It follows then that the difference between $\tilde{p}$ and p_0 is given by

$$\tilde{p}-p_0=\left[\left(\frac{\partial p}{\partial n}\right)_x+\left(\frac{\partial p}{\partial x}\right)_n\frac{d\tilde{x}}{dn}\right]\Delta n. \tag{3.8}$$

A similar argument [now using Eq. (3.6) to relate $x-x_0$ and $\tilde{x}-x_0$] gives the following expression for $p-p_0$:

$$p-p_0=\left[\left(\frac{\partial p}{\partial n}\right)_x+\frac{1}{1-i\hat{\omega}\tau}\left(\frac{\partial p}{\partial x}\right)_n\frac{d\tilde{x}}{dn}\right]\Delta n. \tag{3.9}$$

Combining Eqs. (3.8) and (3.9) gives us an expression for the difference in the pressure $p-\tilde{p}$ that appears on the left side of Eq. (3.1):

$$p-\tilde{p}=\frac{i\hat{\omega}\tau}{1-i\hat{\omega}\tau}\left(\frac{\partial p}{\partial x}\right)_n\frac{d\tilde{x}}{dn}\Delta n. \tag{3.10}$$

Then equating this expression for the left side of Eq. (3.1) with the expression for the right side from Eq. (3.2), we find the desired formula for the bulk viscosity:

$$\zeta=\frac{-n\tau}{1-i\hat{\omega}\tau}\left(\frac{\partial p}{\partial x}\right)_n\frac{d\tilde{x}}{dn}. \tag{3.11}$$

Finally it is convenient to re-express the thermodynamic derivatives that appear in Eq. (3.11) in terms of the more familiar

$$\gamma_\infty=\frac{n}{p}\left(\frac{\partial p}{\partial n}\right)_x, \tag{3.12}$$

the ''infinite'' frequency adiabatic index, and

$$\gamma_0=\frac{n}{p}\left[\left(\frac{\partial p}{\partial n}\right)_x+\left(\frac{\partial p}{\partial x}\right)_n\frac{d\tilde{x}}{dn}\right], \tag{3.13}$$

the ''zero'' frequency adiabatic index. In terms of these quantities, then the bulk viscosity may be written in the form:

$$\zeta=\frac{p(\gamma_\infty-\gamma_0)\tau}{1-i\hat{\omega}\tau}. \tag{3.14}$$

For a fluid composed of particles with non-relativistic energies this expression is equivalent to the conventional one [12] written in terms of the sound speed u, since $p\gamma=\rho u^2$ for such fluids. However for a fluid containing particles with relativistic energies, the conventional form is wrong and Eq. (3.14) is the appropriate form to use. Note that this new form of the bulk viscosity is needed to describe any fluid containing relativistic internal particle energies, even if the bulk motion of the fluid itself has only non-relativistic velocities which are well approximated by Newtonian hydrodynamics. We also see that for a fixed-frequency perturbation, the greatest bulk viscosity comes from processes with relaxation times $\tau\approx 1/\hat{\omega}$. The importance of this fact will become apparent as we examine how the relaxation time τ varies inside a neutron star.

The standard approach [12] to treating multiple reactions is to repeat the preceding derivation for multiple degrees of freedom x_i and relaxation times τ_i. However, this only works if (as in air) the x_i can be chosen to be independent. This is not possible in neutron-star matter, since the degrees of freedom (e.g., concentrations of various baryons) are related to each other even out of thermodynamic equilibrium by constraints such as conservation of baryon number. The reactions of interest to us here are the non-leptonic weak interactions

$$n+n\leftrightarrow p^+ +\Sigma^-,$$

$$n+p^+\leftrightarrow p^+ +\Lambda.$$

Given the microscopic reaction rates for these processes (which are calculated in Sec. IV), we can express all of the perturbed quantities in terms of a single one. Since all the hyperon reactions that contribute to bulk viscosity involve neutrons, we choose as our primary variable the number density of neutrons n_n.

Let $x_n=n_n/n_B$ be the fraction of baryons in a given fluid element that are neutrons. This variable changes only by internal reactions, not directly by changing the volume of the fluid element, and so we can write

$$(\partial_t+\vec{v}\cdot\vec{\nabla})x_n=-(x_n-\tilde{x}_n)/\tau=-\Gamma_n/n_B. \tag{3.15}$$

Here Γ_n is the production rate of neutrons per unit volume, which is proportional to the overall chemical potential imbalance $\delta\mu\equiv\mu-\tilde{\mu}$ (see below). (We normalize n_n and Γ_n to the baryon number density n_B to remove the oscillating time dependence of the volume of the fluid element.) Assuming the reactions described in Sec. IV, the relaxation time is then given by

$$\frac{1}{\tau}=\frac{\Gamma_\Lambda+2\Gamma_\Sigma}{\delta\mu}\frac{\delta\mu}{n_B\delta x_n}, \tag{3.16}$$

where $\delta x_n\equiv x_n-\tilde{x}_n$.

We obtain $\delta\mu/\delta x_n$ from the following constraints:

$$0 = \delta x_n + \delta x_\Lambda + \delta x_p + \delta x_\Sigma , \tag{3.17}$$

$$0 = \delta x_p - \delta x_\Sigma , \tag{3.18}$$

$$0 = \beta_n \delta x_n + \beta_\Lambda \delta x_\Lambda + \beta_p \delta x_p + \beta_\Sigma \delta x_\Sigma , \tag{3.19}$$

where x_i are the number densities of baryon species normalized to the total number density of baryons and the β_i are defined below. The first constraint is conservation of baryon number, obeyed by all reactions. (We note that since $\delta n_B = n_B - \tilde{n}_B \equiv 0$, $\delta x_i = \delta n_i / n_B$.) The second constraint is related to conservation of electric charge, but is stricter: We assume that all leptonic (Urca) reaction rates are much smaller than those which produce hyperon bulk viscosity and so protons are only produced in reactions that produce a Σ^-. The third constraint is that the non-leptonic reaction

$$n + \Lambda \leftrightarrow p^+ + \Sigma^- \tag{3.20}$$

proceeds much faster than the weak interactions which produce hyperon bulk viscosity since it is mediated by the strong nuclear interaction. Here we use the shorthand

$$\alpha_{ij} = \left(\frac{\partial \mu_i}{\partial n_j} \right)_{n_k, k \neq j} , \tag{3.21}$$

$$\beta_i = \alpha_{ni} + \alpha_{\Lambda i} - \alpha_{pi} - \alpha_{\Sigma i} . \tag{3.22}$$

Equilibrium with respect to reaction (3.20) ensures that both processes described in Sec. IV have the same chemical potential imbalance,

$$\delta\mu \equiv \delta\mu_n - \delta\mu_\Lambda = 2\delta\mu_n - \delta\mu_p - \delta\mu_\Sigma . \tag{3.23}$$

It is straightforward then to express $\delta\mu$ in terms of the δx_i, and then to eliminate all but δx_n using the constraints Eqs. (3.17)–(3.19). The result

$$\frac{\delta\mu}{n_B \delta x_n} = \alpha_{nn} + \frac{(\beta_n - \beta_\Lambda)(\alpha_{np} - \alpha_{\Lambda p} + \alpha_{n\Sigma} - \alpha_{\Lambda\Sigma})}{2\beta_\Lambda - \beta_p - \beta_\Sigma} - \alpha_{\Lambda n} - \frac{(2\beta_n - \beta_p - \beta_\Sigma)(\alpha_{n\Lambda} - \alpha_{\Lambda\Lambda})}{2\beta_\Lambda - \beta_p - \beta_\Sigma} , \tag{3.24}$$

then determines via Eq. (3.16) the relaxation time that appears in the bulk viscosity formula Eq. (3.14). For a certain range of densities there are Σ^- hyperons present in Glendinning's equation of state, but no Λ. In that case the variable δx_Λ remains zero, and the constraint Eq. (3.19) is no longer enforced. In this case the chemical potential imbalance can still be expressed in terms of δx_n with the somewhat simpler result

$$\frac{2\delta\mu}{n_B \delta x_n} = 4\alpha_{nn} - 2(\alpha_{pn} + \alpha_{\Sigma n} + \alpha_{np} + \alpha_{n\Sigma}) + \alpha_{pp} + \alpha_{\Sigma p} + \alpha_{p\Sigma} + \alpha_{\Sigma\Sigma} . \tag{3.25}$$

The equation of state of neutron-star matter is generally written in a form which gives the thermodynamic variables as functions of the various particle species present, e.g. the pressure would be specified as $p = p(n_i)$. In order to evaluate the thermodynamic derivatives $(\partial p/\partial n)_x$ and $(\partial p/\partial x)_n$ that are needed in Eq. (3.11), we note that $n_n = n_B x_n$ for our choice of x. Thus the partial derivative needed in Eq. (3.11) is given by $(\partial p/\partial x)_n = n_B \partial p/\partial n_n$. Similarly, if needed, $(\partial p/\partial n)_x = \Sigma_i x_i \partial p/\partial n_i$. The derivative $d\tilde{x}/dn$ that also appears in Eq. (3.11) is determined by constructing a sequence of complete equilibrium models (e.g. by imposing all of the necessary β-equilibrium constraints, etc.) for different total baryon number densities n_B. This complete model of the equilibrium states will include the functions $\tilde{x}_n(n_B)$, from which the derivative $d\tilde{x}_n/dn_B$ is easily computed.

Formation of a superfluid (of a given particle species) is marked by the formation of Cooper pairs and collapse of the pairs into a Bose-Einstein condensate. It is the unpaired particles that we are concerned with, since they are the ones that can participate in the bulk-viscosity generating reactions. The free-particle states within the pair-binding energy Δ of the Fermi surface are depleted. As a result all phase-space factors (and effectively the reaction rates) are decreased by roughly a factor $e^{-\Delta/kT}$. The effect of superfluidity can be included in our ordinary-fluid bulk viscosity calculation then simply by making the substitution

$$\Gamma \rightarrow e^{-\Delta/kT} \Gamma . \tag{3.26}$$

Thus when superfluidity is taken into account the equation for the relaxation time, Eq. (3.16) becomes

$$\frac{1}{\tau} = \left(\frac{\Gamma_\Lambda}{\delta\mu} e^{-\Delta_\Lambda/kT} + \frac{2\Gamma_\Sigma}{\delta\mu} e^{-\Delta_\Sigma/kT} \right) \frac{\delta\mu}{n_B \delta x_n} . \tag{3.27}$$

IV. MICROSCOPIC REACTION RATES

Since the Σ^- and Λ hyperons form at the lowest threshold densities, we are most interested in the nonleptonic reactions forming them from neutrons. Following Jones' earlier work [2,4] we calculate rates for two reactions,

$$n + n \leftrightarrow p^+ + \Sigma^- , \tag{4.1}$$

$$n + p^+ \leftrightarrow p^+ + \Lambda , \tag{4.2}$$

as tree-level Feynman diagrams involving the exchange of a W boson. In his most recent paper [3], Jones treats the reaction

$$n + n \leftrightarrow n + \Lambda , \tag{4.3}$$

which is generally the dominant channel for Λ production in laboratory experiments on hypernuclei. This process has no simple W-exchange contribution. Several other processes contribute, but at present the rate cannot be well predicted from theory. Some of these processes surely operate in reactions (4.1) and (4.2) and modify the rates, perhaps signifi-

cantly. However, our simple calculations should provide a reasonable lower limit on the rates and thus an upper limit on the bulk viscosity.

A. Single reactions

We calculate reaction rates using the standard techniques of time-dependent perturbation theory in relativistic quantum mechanics. We use the conventions of Griffiths [16]: spinors are normalized to $\overline{u}u=2m$, the fifth Dirac matrix is $\gamma^5=i\gamma^0\gamma^1\gamma^2\gamma^3$, the metric has negative trace, and $\hbar=1$. For a single reaction (4.1) or (4.2) between particles with 4-momenta p_i, the differential reaction rate (number per unit volume per unit time) is

$$d\Gamma=|\mathcal{M}|^2(2\pi)^4\delta^{(4)}(p_1+p_2-p_3-p_4)S\prod_{i=1}^{4}\frac{d^3\boldsymbol{p}_i}{(2\pi)^3 2\epsilon_i}, \tag{4.4}$$

where $|\mathcal{M}|^2$ is the spinor matrix element (squared and summed over spin states), boldface $\boldsymbol{p}_i$ are 3-momenta, and ϵ_i are particle energies. The statistical factor S, which compensates for overcounting momentum states of indistinguishable particles, is 1/2 for reaction (4.1) and 1 for reaction (4.2).

First, consider the Λ reaction (4.2), which we represent by a single tree-level diagram. Labeling the particles 1 (neutron), 2 (ingoing proton), 3 (outgoing proton), 4 (Λ hyperon), we obtain the matrix element (for a single set of spin states)

$$\mathcal{M}_\Lambda=\frac{G_F}{2\sqrt{2}}\sin 2\theta_C[\overline{u}(p_3)\gamma^\mu(1+g_{np}\gamma^5)u(p_1)\overline{u}(p_4)\times\gamma_\mu(1+g_{p\Lambda}\gamma^5)u(p_2)]. \tag{4.5}$$

Here G_F is the Fermi coupling constant and θ_C is the Cabibbo weak mixing angle. The quantities g_{np}, $g_{n\Sigma}$, and $g_{p\Lambda}$ are axial-vector couplings (normalized to the vector coupling) of the weak interaction, whose deviation from -1 represents the partial nonconservation of the axial current. (These quantities are often written g_A or G_A/G_V in the particle and nuclear physics literature. We add a label to keep track of which nucleon-hyperon line is which.) We use the values $G_F=1.166\times10^{-11}$ MeV^{-2} and $\sin\theta_C=0.222$ from the Particle Data Group [17]. The axial-vector couplings change with varying momentum transfer and density of the medium in a way that reflects the internal (strong-interaction) structure of the baryons and is therefore difficult to calculate. We use the values $g_{np}=-1.27$, $g_{p\Lambda}=-0.72$, and $g_{n\Sigma}=0.34$ measured in β-decay of baryons at rest [17]. There are theoretical reasons to believe that all axial-vector couplings tend to their asymptotically free values of -1 in a dense medium [18]. We provide dissipation numbers in later sections both for laboratory values and for asymptotic values of the couplings to give an estimate of the uncertainty in this calculation.

To obtain the net reaction rate Γ we sum $|\mathcal{M}|^2$ over all possible initial and final spin states. This is done in the standard way by tracing over outer products of spinors:

$$\begin{aligned}|\mathcal{M}_\Lambda|^2=4G_F^2\sin^2 2\theta_C\{&2m_n m_p^2 m_\Lambda(1-g_{np}^2)(1-g_{p\Lambda}^2)\\&-m_n m_p p_2\cdot p_4(1-g_{np}^2)(1+g_{p\Lambda}^2)\\&-m_p m_\Lambda p_1\cdot p_3(1+g_{np}^2)(1-g_{p\Lambda}^2)\\&+p_1\cdot p_2 p_3\cdot p_4[(1+g_{np}^2)(1+g_{p\Lambda}^2)+4g_{np}g_{p\Lambda}]\\&+p_1\cdot p_4 p_2\cdot p_3[(1+g_{np}^2)(1+g_{p\Lambda}^2)-4g_{np}g_{p\Lambda}]\},\end{aligned} \tag{4.6}$$

which in the low-momentum limit used by Jones [3] reduces to

$$|\mathcal{M}_\Lambda|^2=8G_F^2\sin^2 2\theta_C m_n m_p^2 m_\Lambda(1+3g_{np}^2 g_{p\Lambda}^2). \tag{4.7}$$

Note that this limit corresponds to $G_\Lambda=0.40G_F$ in the notation of Jones [3], who obtains $G_\Lambda=1.29G_F$. The factor of 3 discrepancy is within the uncertainties of modern nuclear-matter physics, as we see by, e.g., taking the asymptotic values of the axial-vector couplings.

Reaction (4.1) is treated similarly, with particle labels 1 and 2 (neutrons), 3 (proton), and 4 (Σ^- hyperon). Antisymmetrizing with respect to the two indistinguishable neutrons, the matrix element is

$$\begin{aligned}\mathcal{M}_\Sigma=\frac{G_F}{2\sqrt{2}}\sin 2\theta_C&\overline{u}(p_3)\gamma^\mu(1+g_{np}\gamma^5)[u(p_1)\overline{u}(p_4)\\&\times\gamma_\mu(1+g_{n\Sigma}\gamma^5)u(p_2)-u(p_2)\overline{u}(p_4)\gamma_\mu(1+g_{n\Sigma}\gamma^5)\\&\times u(p_1)].\end{aligned} \tag{4.8}$$

The squared sum over spins is given by

$$\begin{aligned}|\mathcal{M}_\Sigma|^2=4G_F^2\sin^2 2\theta_C\{&6m_n^2 m_p m_\Sigma(1-g_{np}^2)(1-g_{n\Sigma}^2)-m_p m_\Sigma p_1\cdot p_2(1-g_{np}^2)(1-g_{n\Sigma}^2)-2m_n m_\Sigma p_1\cdot p_3(1+g_{np}^2)(1-g_{n\Sigma}^2)\\&-2m_n m_p p_1\cdot p_4(1-g_{np}^2)(1+g_{n\Sigma}^2)-2m_n m_\Sigma p_2\cdot p_3(1+g_{np}^2)(1-g_{n\Sigma}^2)-2m_n m_p p_2\cdot p_4(1-g_{np}^2)(1+g_{n\Sigma}^2)\\&-m_n^2 p_3\cdot p_4[(1+g_{np}^2)(1+g_{n\Sigma}^2)-4g_{np}g_{n\Sigma}]+4p_1\cdot p_2 p_3\cdot p_4[(1+g_{np}^2)(1+g_{n\Sigma}^2)+4g_{np}g_{n\Sigma}]+p_1\cdot p_3 p_2\cdot p_4\\&\times[(1+g_{np}^2)(1+g_{n\Sigma}^2)-4g_{np}g_{n\Sigma}]+p_1\cdot p_4 p_2\cdot p_3[(1+g_{np}^2)(1+g_{n\Sigma}^2)-4g_{np}g_{n\Sigma}]\},\end{aligned} \tag{4.9}$$

which in the low-momentum limit reduces to

$$|\mathcal{M}_\Sigma|^2 = 8 G_F^2 \sin^2 2\theta_C m_n^2 m_p m_\Sigma (1+3g_{np}g_{n\Sigma})^2. \tag{4.10}$$

This expression agrees with Eq. (7) of Jones' old paper [4], allowing for our different placement of the statistical overcounting factor and different normalization of the spinors (he uses $\overline{uu}=1$). However, we find that for this reaction the low-momentum limit is a very poor approximation to the full result: the collision integral computed in the next subsection can be more than an order of magnitude higher than Eq. (4.10) would suggest. This effectively brings down the coefficient of bulk viscosity ζ by a factor of about 5 at densities $(5-6)\times 10^{14}$ g/cm^3, where there are no Λ hyperons [19].

B. Collision integrals

Reactions (4.1) and (4.2) can be regarded as scattering processes wherein the scattered particles change identity. Therefore we can use existing results on collision integrals in the literature on superfluidity (e.g., [20]) with some slight modifications. We now integrate the differential reaction rate (4.4) over momentum space to obtain the total rate

$$\Gamma = \frac{S}{4096\pi^8}\int \prod_{i=1}^{4}\frac{d^3\boldsymbol{p}_i}{\epsilon_i}|\mathcal{M}|^2\delta^{(3)}(\boldsymbol{p}_1+\boldsymbol{p}_2-\boldsymbol{p}_3-\boldsymbol{p}_4) \times F(\epsilon_i)\,\delta(\epsilon_1+\epsilon_2-\epsilon_3-\epsilon_4). \tag{4.11}$$

(From here on we use italic p_i to denote the absolute value of the 3-momenta, $p_i=\sqrt{\boldsymbol{p}_i\cdot\boldsymbol{p}_i}$.) The Pauli blocking factor

$$F(\epsilon_i) = f_1 f_2 (1-f_3)(1-f_4) - (1-f_1)(1-f_2) f_3 f_4, \tag{4.12}$$

where

$$f_i = 1/\{1+\exp[(\epsilon_i-\mu_i)/kT]\}, \tag{4.13}$$

accounts for the degeneracy of the reactant particles and restricts the available phase space to those particles within roughly kT of their Fermi energies.

In the case where all particles are degenerate (which is true except for a very small region just above the threshold density for each hyperon species), the collision integral separates into angular and energetic parts. The energetic part can be written in the limit $\delta\mu \ll kT$ as

$$\int \prod_i d\epsilon_i F(\epsilon_i)\,\delta(\epsilon_1+\epsilon_2-\epsilon_3-\epsilon_4) = (kT)^2\delta\mu\int_{-\infty}^{+\infty}\frac{y^2 dy}{(e^y-1)(1-e^{-y})}, \tag{4.14}$$

where the latter integral has the value $2\pi^2/3$.

We address the angular integral with the aid of Fig. 7. With no preferred direction (e.g., strong magnetic field), the $\boldsymbol{p}_1$ volume element is $4\pi p_1^2 dp_1$ and the $\boldsymbol{p}_2$ volume element is $p_2^2 dp_2 \sin\theta d\theta d\phi$, where θ and ϕ are the polar and azimuthal angles of $\boldsymbol{p}_2$ with respect to $\boldsymbol{p}_1$. Conservation of momentum demands that $\boldsymbol{p}_1+\boldsymbol{p}_2=\boldsymbol{p}_3+\boldsymbol{p}_4$, determining a common axis. Let α and α' be the angles of $\boldsymbol{p}_1$ and $\boldsymbol{p}_3$ with that axis. The volume element of $\boldsymbol{p}_3$ is then $p_3\sin\alpha' d\alpha' d\phi'$, where ϕ' is the angle between $\boldsymbol{p}_1\times\boldsymbol{p}_2$ and $\boldsymbol{p}_3\times\boldsymbol{p}_4$, multiplied by the area element in the plane containing $\boldsymbol{p}_3$ and $\boldsymbol{p}_4$. To separate the energetic and angular integrals, it is convenient to write this area element as $dp_3 dp_4/\sin\theta'$, where θ' is the angle between $\boldsymbol{p}_3$ and $\boldsymbol{p}_4$. Before leaving Fig. 7, note the following useful identities:

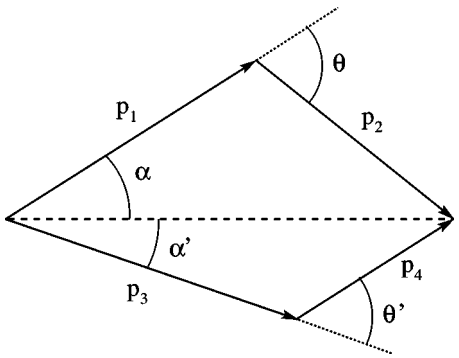

FIG. 7. Definition of angles used in the collision integral. The plane containing $\boldsymbol{p}_3$ and $\boldsymbol{p}_4$ can be rotated out of the page around the long-dashed common axis by an angle ϕ' for a given $\boldsymbol{p}_1$ and $\boldsymbol{p}_2$.

$$p_1^2+p_2^2+2p_1p_2\cos\theta = p_3^2+p_4^2+2p_3p_4\cos\theta', \tag{4.15}$$

$$p_1\sin\alpha = p_2\sin(\theta-\alpha), \tag{4.16}$$

$$p_3\sin\alpha' = p_4\sin(\theta'-\alpha'). \tag{4.17}$$

We use the differential of the first identity (with p_i held constant) to write our final result for the volume element as

$$\delta^{(3)}(\boldsymbol{p}_1+\boldsymbol{p}_2-\boldsymbol{p}_3-\boldsymbol{p}_4)\prod_{i=1}^{4}\frac{d^3\boldsymbol{p}_i}{\epsilon_i} = 4\pi p_3\sin\alpha' d\theta' d\phi' \times d\phi\prod_{i=1}^{4} d\epsilon_i. \tag{4.18}$$

Although ϕ and ϕ' are free to range from 0 to 2π, the limits of integration over θ' depend on the relations between the momenta p_i, which are constrained to be close to the Fermi momenta. (Therefore from now on we use p_i to refer to the Fermi momenta.) We integrate θ' over the full range 0 to π, which is allowed by momentum conservation for

$$p_n \geqslant p_p \geqslant (p_\Lambda, p_\Sigma), \quad p_n - p_p \leqslant p_p - p_\Lambda. \tag{4.19}$$

In our equation of state these Fermi momentum criteria are satisfied for $\rho < 1.0\times 10^{15}$ g/cm^3 (see Fig. 1). It turns out that almost all of the dissipation takes place below this density, and much above this density the baryons are too closely

packed to maintain their separate identities anyway. Therefore for our purposes it is sufficient to treat only the case (4.19).

Now consider the case that $|\mathcal{M}|^2$ does not depend on any of the angles, such as in the limit $p_i/m_i \ll 1$. We can integrate trivially over all the angles, with the exception of

$$\int_0^\pi p_3 \sin\alpha' d\theta' = 2p_4, \tag{4.20}$$

where p_4 is the smallest (i.e., hyperon) Fermi momentum involved. This motivates us to use Eq. (4.14) to write

$$\Gamma = \frac{S}{192\pi^3}\langle|\mathcal{M}|^2\rangle p_4 (kT)^2 \delta\mu, \tag{4.21}$$

where $\langle|\mathcal{M}|^2\rangle$ is the angle-averaged value of $|\mathcal{M}|^2$. We write $|\mathcal{M}|^2$ in terms of the integrals

$$\langle \boldsymbol{p}_1\cdot\boldsymbol{p}_2\rangle = \frac{1}{6}(-3p_1^2-3p_2^2+3p_3^2+p_4^2), \tag{4.22}$$

$$\langle \boldsymbol{p}_1\cdot\boldsymbol{p}_3\rangle = \frac{1}{6}(-3p_1^2+3p_2^2-3p_3^2+p_4^2), \tag{4.23}$$

$$\langle \boldsymbol{p}_1\cdot\boldsymbol{p}_4\rangle = \langle \boldsymbol{p}_2\cdot\boldsymbol{p}_4\rangle = \langle \boldsymbol{p}_3\cdot\boldsymbol{p}_4\rangle = -\frac{1}{3}p_4^2, \tag{4.24}$$

$$\langle \boldsymbol{p}_2\cdot\boldsymbol{p}_3\rangle = \frac{1}{6}(3p_1^2-3p_2^2-3p_3^2+p_4^2), \tag{4.25}$$

$$\langle \boldsymbol{p}_1\cdot\boldsymbol{p}_2\,\boldsymbol{p}_3\cdot\boldsymbol{p}_4\rangle = \frac{1}{30}p_4^2(5p_1^2+5p_2^2+5p_3^2-p_4^2), \tag{4.26}$$

$$\begin{aligned}\langle \boldsymbol{p}_1\cdot\boldsymbol{p}_3\,\boldsymbol{p}_2\cdot\boldsymbol{p}_4\rangle &= \langle \boldsymbol{p}_1\cdot\boldsymbol{p}_4\,\boldsymbol{p}_2\cdot\boldsymbol{p}_3\rangle \\ &= \frac{p_4^2}{60(p_3^2-p_4^2)}[5p_1^4-10p_1^2p_2^2+5p_2^2 \\ &\quad +3(5p_3^4-6p_3^2p_4^2+p_4^4)].\end{aligned} \tag{4.27}$$

(Note that some dot products, e.g., $\boldsymbol{p}_1\cdot\boldsymbol{p}_3$, depend on ϕ'. The average over ϕ' is then nontrivial but is easily taken by symmetry about the common axis.)

The results for the angle averages are

$$\begin{aligned}\langle|\mathcal{M}_\Lambda|^2\rangle = \frac{G_F^2\sin^2 2\theta_C}{15}&(120(1-g_{np}^2)(1-g_{p\Lambda}^2)m_n m_p^2 m_\Lambda \\ &-20(1-g_{np}^2)(1+g_{p\Lambda}^2)m_n m_p(3\epsilon_p\epsilon_\Lambda - p_\Lambda^2) \\ &-10(1+g_{np}^2)(1-g_{p\Lambda}^2)m_p m_\Lambda(6\epsilon_n\epsilon_p - 3p_n^2 \\ &+p_\Lambda^2)+2[(1+g_{np}^2)(1+g_{p\Lambda}^2)+4g_{np}g_{p\Lambda}] \\ &\times[5\epsilon_p\epsilon_\Lambda(6\epsilon_n\epsilon_p+3p_n^2-p_\Lambda^2)+p_\Lambda^2(10\epsilon_n\epsilon_p+5p_n^2 \\ &+10p_p^2-p_\Lambda^2)]+[(1+g_{np}^2)(1+g_{p\Lambda}^2)-4g_{np}g_{p\Lambda}] \\ &\times\{10\epsilon_n\epsilon_\Lambda(6m_p^2+3p_n^2+p_\Lambda^2)+p_\Lambda^2[-20\epsilon_p^2 \\ &+15p_p^2-3p_\Lambda^2+5(p_n^2-p_p^2)^2/(p_p^2-p_\Lambda^2)]\}).\end{aligned} \tag{4.28}$$

[Note that the denominator in the last term does not diverge while criterion (4.19) holds.] Similarly, for reaction (4.1),

$$\begin{aligned}\langle|\mathcal{M}_\Sigma|^2\rangle = \frac{2}{15}G_F^2\sin^2 2\theta_C&\{180(1-g_{np}^2)(1-g_{n\Sigma}^2)m_n^2 m_p m_\Sigma \\ &-40(1-g_{np}^2)(1+g_{n\Sigma}^2)m_n m_p(3\epsilon_n\epsilon_\Sigma - p_\Sigma^2) \\ &-20(1+g_{np}^2)(1-g_{n\Sigma}^2)m_n m_\Sigma(6\epsilon_n\epsilon_p - 3p_p^2+p_\Sigma^2) \\ &-5(1-g_{np}^2)(1-g_{n\Sigma}^2)m_p m_\Sigma(6\epsilon_n^2+6p_n^2-3p_p^2 \\ &-p_\Sigma^2)+4[(1+g_{np}^2)(1+g_{n\Sigma}^2)+4g_{np}g_{n\Sigma}] \\ &\times[10\epsilon_n^2(3\epsilon_p\epsilon_\Sigma+p_\Sigma^2)+5\epsilon_p\epsilon_\Sigma(6p_n^2-3p_p^2-p_\Sigma^2) \\ &+p_\Sigma^2(10p_n^2+5p_p^2-p_\Sigma^2)]+10[(1+g_{np}^2)(1+g_{n\Sigma}^2) \\ &-4g_{np}g_{n\Sigma}][-m_n^2(3\epsilon_p\epsilon_\Sigma+p_\Sigma^2)+\epsilon_n(6\epsilon_n\epsilon_p\epsilon_\Sigma \\ &-2\epsilon_p p_\Sigma^2-3\epsilon_\Sigma p_p^2+\epsilon_\Sigma p_\Sigma^2)]\}.\end{aligned} \tag{4.29}$$

These angle averages are inserted into Eq. (4.21) to yield the net reaction rate per unit volume as a function of Fermi momenta.

V. RELAXATION TIMES

The relaxation time scales for the non-leptonic weak interactions, Eqs. (4.1) and (4.2), can now be determined by combining the microscopic collision rates determined in Sec. IV with the thermodynamic quantities evaluated in Secs. II and III. At densities above the threshold for the production of Σ^-, but below the Λ threshold, the final expression for the relaxation time scale τ is

$$\frac{1}{\tau} = \frac{(kT)^2}{192\pi^3}\frac{p_\Sigma\langle|\mathcal{M}_\Sigma|^2\rangle}{e^{\Delta_\Sigma/kT}}\frac{\delta\mu}{n_B\delta x_n}. \tag{5.1}$$

Here the collision cross section $|\mathcal{M}_\Sigma|^2$ is evaluated from Eq. (4.29). The Fermi momenta that appear in this expression are obtained from the complete description of the equilibrium thermodynamic state as described in Sec. II. This description includes the values of the particle densities (and hence Fermi

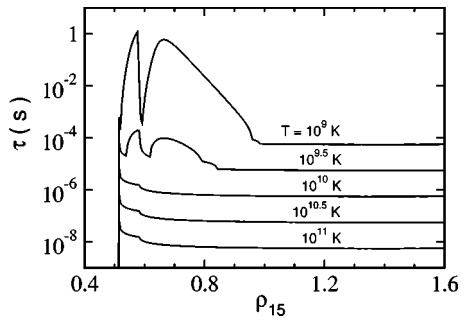

FIG. 8. Density dependence (in units of 10^{15} g/cm^3) of the relaxation time scale τ (in units of s) for a range of temperatures. These curves were constructed using the assumption $\Delta_{\Sigma^-}=\Delta_\Lambda$ for the Σ^- superfluid gap.

momenta) of each species as a function of the total baryon density. The thermodynamic quantity $\delta\mu/n_B\delta x_n$ is given by Eq. (3.25) in terms of chemical potentials and their derivatives. Once the density increases to the point that both Σ^- and Λ hyperons are present in the equilibrium state, then the expression for the relaxation time scale becomes

$$\frac{1}{\tau}=\frac{(kT)^2}{192\pi^3}\left[\frac{p_\Sigma\langle|\mathcal{M}_\Sigma|^2\rangle}{e^{\Delta_\Sigma/kT}}+\frac{p_\Lambda\langle|\mathcal{M}_\Lambda|^2\rangle}{e^{\Delta_\Lambda/kT}}\right]\frac{\delta\mu}{n_B\delta x_n}. \quad (5.2)$$

Here the collision cross sections are given by Eqs. (4.28) and (4.29), and $\delta\mu/n_B\delta x_n$ is given by Eq. (3.24) in this case.

We have evaluated this relaxation time scale for neutron-star matter using the equation of state described in Sec. II. Figure 8 illustrates the density dependence of this time scale for a range of temperatures. In the case of Fig. 8 we have assumed that the Σ^- superfluid gap function is given by $\Delta_\Sigma=\Delta_\Lambda$, while in Fig. 9 we assume $\Delta_\Sigma=10\Delta_\Lambda$. The only significant difference between these two cases comes about in the density range where there exist Σ^- but not Λ. In that range the time scale is significantly increased in the $\Delta_\Sigma=10\Delta_\Lambda$ case by the stronger superfluid effects. All of the curves in these two figures were evaluated using the ''standard'' β-decay values of the axial-vector coupling constants: $g_{np}=-1.27$, $g_{p\Lambda}=-0.72$, and $g_{n\Sigma}=0.34$ [17] and the effective masses of all of the baryons when evaluating the scattering cross sections. There are theoretical arguments that

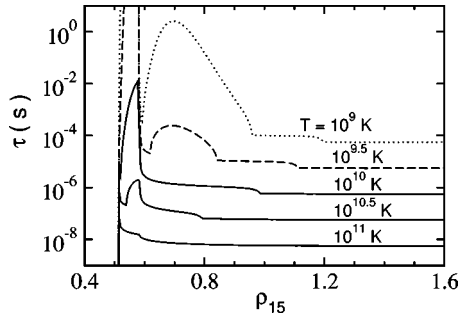

FIG. 9. Density dependence (in units of 10^{15} g/cm^3) of the relaxation time scale τ (in units of s) for a range of temperatures. These curves were constructed using the assumption $\Delta_{\Sigma^-}=10\Delta_\Lambda$ for the Σ^- superfluid gap.

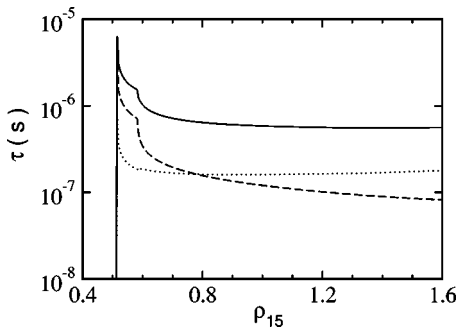

FIG. 10. Density dependence (in units of 10^{15} g/cm^3) of the relaxation time scale τ (in units of s) for $T=10^{10}$ K. Solid curve uses effective masses and the β-equilibrium values of the axial-vector couplings. Other curves explore various alternate microphysics assumptions: dashed curve uses bare masses, dotted curve uses $g_B=-1$.

suggest the coupling constants should approach the values $g_{np}=g_{p\Lambda}=g_{n\Sigma}=-1$ in a dense medium [18]. We illustrate the impact this might have on these time scales in Fig. 10 (dotted curve). We also illustrate in this figure (dashed curve) the effect of using the bare masses of the various baryons when computing the scattering cross sections. We see that the overall effect of these changes is to make the time scales shorter (by up to an order of magnitude). This tends to decrease the bulk viscosity by a similar factor, until the temperature drops below the superfluid critical values.

Finally, we are in a position now to evaluate the bulk viscosity itself. The real part of the bulk viscosity, the part that is responsible for damping the modes of neutron stars, is given by the expression

$$\mathrm{Re}\,\zeta=\frac{p(\gamma_\infty-\gamma_0)\tau}{1+(\hat{\omega}\tau)^2}. \quad (5.3)$$

Figures 11 and 12 illustrate the density and temperature dependence of ζ. (Here we assume that the frequency corresponds to the $m=2$ r-mode frequency of a maximally rotating neutron star: $\hat{\omega}=\frac{2}{3}\Omega_{\max}$.) These figures illustrate the complicated temperature dependence of the visocity due to superfluid effects. For temperatures slightly below the super-

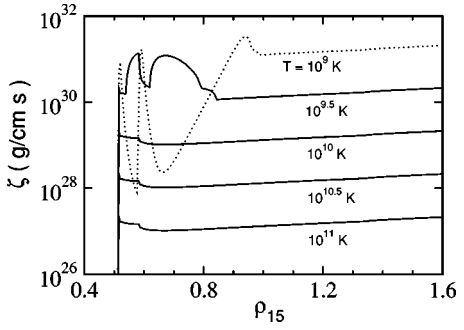

FIG. 11. Density dependence (in units of 10^{15} g/cm^3) of the hyperon bulk viscosity (in units of g/cm s) for a range of temperatures. These curves were constructed using the assumption $\Delta_{\Sigma^-}=\Delta_\Lambda$ for the Σ^- superfluid gap.

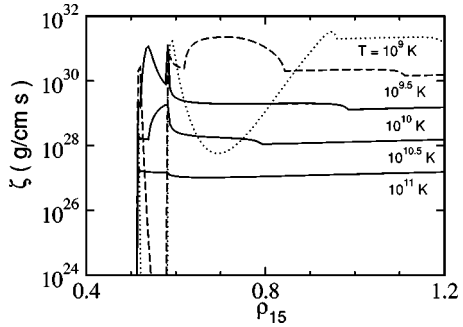

FIG. 12. Density dependence (in units of 10^{15} g/cm^3) of the hyperon bulk viscosity (in units of g/cm s) for a range of temperatures. These curves were constructed using the assumption $\Delta_{\Sigma^-}=10\Delta_\Lambda$ for the Σ^- superfluid gap.

fluid critical temperature the values of the bulk viscosity are increased over their normal values. This is due to an increase in the time scale τ which moves it closer to being in resonance with the pulsation period of the mode. Once the temperature falls well below the superfluid critical temperature however, we see that the time scale τ becomes even longer than the pulsation period and so the viscosity becomes smaller again in this case. We note that even for very low temperatures there exists a small range of densities, just above the hyperon threshold densities, where the bulk viscosity remains rather large. This is due to the momentum dependence of the superfluid gap, Eq. (2.7). The gap Δ goes to zero as the Fermi momentum of the particle goes to zero. Thus just above the threshold density the superfluid gap vanishes (for any finite temperature) so the material in this region will retain the normal-fluid value of the bulk viscosity.

Our value of ζ is generally much larger than that obtained recently by Jones [3]: at a total density $\rho=7\times10^{14}$ g/cm^3 and temperature $T=10^{10}$ K, our ζ is larger than Jones' by a factor of 400. Roughly a factor of 8 is due to the relatively weak coupling we calculate for reaction in Eq. (4.2). (At this density the Σ^- hyperons account for only about 10% of the bulk viscosity and can be neglected.) We note that using the asymptotic values of the weak axial-vector couplings would erase much of this factor of 8 difference, and thus it is indicative of the size of the uncertainties in ζ due to our poor understanding of nuclear-matter physics. The remaining factor of 50 is thermodynamic in origin. Jones evaluates various partial derivatives of pressure and chemical potentials, e.g., appearing in Eq. (3.24) of our paper and Eq. (42) of Ref. [3], using the values for a gas of noninteracting fermions. We include all the mesonic interaction terms, whose effect is to increase significantly these thermodynamic derivatives. Since the details of the neutron-star equation of state are uncertain, the precise values of the derivatives are correspondingly uncertain. However, we think it unlikely that the true physical mesonic terms will cancel precisely enough to bring the derivatives down to their noninteracting values. In summary, we think that the true value of ζ is within an order of magnitude of the value we compute here.

VI. *r*-MODE DAMPING TIMES

The basic formalism for evaluating the effects of bulk viscosity on the stability of the *r*-modes is well known [9,21]. The time derivative of the co-rotating frame energy $\tilde{E}$ due to the effects of bulk viscosity is

$$\frac{d\tilde{E}}{dt}=-\int \mathrm{Re}\,\zeta|\vec{\nabla}\cdot\delta\vec{v}|^2d^3x. \tag{6.1}$$

This rotating frame energy $\tilde{E}$ is (to lowest order in the angular velocity of the star) given by the integral

$$\tilde{E}=\frac{1}{2}\int \rho|\delta\vec{v}|^2d^3x. \tag{6.2}$$

The time scale $\tau_{B(h)}$ on which hyperon bulk viscosity damps the mode is then

$$\frac{1}{\tau_{B(h)}}=-\frac{1}{2\tilde{E}}\frac{d\tilde{E}}{dt}. \tag{6.3}$$

Here we have normalized $\tau_{B(h)}$ so that $1/\tau_{B(h)}$ is the hyperon bulk viscosity contribution to the imaginary part of the frequency of the mode.

For the case of the *r*-modes (in slowly rotating stars) the integrals that determine $\tilde{E}$ and $d\tilde{E}/dt$ in Eqs. (6.1) and (6.2) can be reduced to simple one-dimensional integrals. For the case of $\tilde{E}$ this reduction is well known [9]:

$$\tilde{E}=\frac{1}{2}\alpha^2\Omega^2R^{-2}\int_0^R\rho r^6dr. \tag{6.4}$$

Here α represents the dimensionless amplitude of the *r*-mode, and Ω and R are the angular velocity and radius of the star respectively. The reduction of $d\tilde{E}/dt$ to a one-dimensional integral is not so straightforward. In general the expansion of the mode $\vec{\nabla}\cdot\delta\vec{v}$ is a complicated function of radius and angle. To lowest order in slowly rotating stars the bulk viscosity ζ will depend only on radius. Thus we may always convert Eq. (6.1) to a one-dimensional integral by defining the angle averaged expansion squared $\langle|\vec{\nabla}\cdot\delta\vec{v}|^2\rangle$:

$$\frac{d\tilde{E}}{dt}=-4\pi\int_0^R\mathrm{Re}\,\zeta\langle|\vec{\nabla}\cdot\delta\vec{v}|^2\rangle r^2dr. \tag{6.5}$$

While the angle-averaged expansion is in general a complicated function, for the case of the *r*-modes it is rather simple. This function has only been determined numerically [21], however the simple analytical expression,

$$\langle|\vec{\nabla}\cdot\delta\vec{v}|^2\rangle=\frac{\alpha^2\Omega^2}{690}\left(\frac{r}{R}\right)^6\left[1+0.86\left(\frac{r}{R}\right)^2\right], \tag{6.6}$$

is an excellent fit to those numerical solutions.

Once the structure of the density function $\rho(r)$ in a stellar model is determined, it is straightforward to evaluate the integrals in Eqs. (6.4) and (6.5) using Eq. (6.6) to determine the bulk viscosity damping time $\tau_{B(h)}$. The bulk viscosity of interest to us here is very sensitive to the density of hyperons in the stellar core. Thus we use the relativistic stellar struc-

ture equations to evaluate $\rho(r)$. This ensures that the size and structure of the hyperon containing core are sufficiently accurate for our purposes. These functions $\rho(r)$ are illustrated for a range of stellar masses in Fig. 3 based on the equation of state discussed in Sec. II. Given these (numerical) expressions for $\rho(r)$ it is straightforward then to use the expressions for the hyperon bulk viscosity ζ derived in Sec. V to obtain $\zeta(r)$ for any given neutron star temperature. Together $\rho(r)$ and $\zeta(r)$ then determine $\tau_{B(h)}$ through Eqs. (6.4), (6.5) and (6.3). While it is straightforward to evaluate these time scales, the result is a rather complicated function of the temperature, angular velocity, and mass of the stellar model and so we do not attempt to illustrate it directly.

The most important application of the hyperon bulk viscosity time scale $\tau_{B(h)}$ is the analysis of the role this type of dissipation plays in the gravitational radiation driven instability in the *r*-modes. Gravitational radiation contributes a term to the evolution of the energy $d\tilde{E}/dt$ that is positive. As is well known by now, gravitational radiation tends to drive the *r*-modes unstable in all rotating stars [22,23]. As has been discussed in detail elsewhere [9,21] the imaginary part of the frequency of the *r*-mode may be written as

$$\frac{1}{\tau_r} = -\frac{1}{\tau_{GR}} + \frac{1}{\tau_{B(h)}} + \frac{1}{\tau_{B(u)}}. \tag{6.7}$$

Here τ_{GR} represents the time scale for gravitational radiation to effect the *r*-mode, $\tau_{B(h)}$ is the hyperon bulk viscosity time scale discussed here, and $\tau_{B(u)}$ is the modified Urca bulk viscosity. Detailed expressions for evaluating these other terms are discussed elsewhere and will not be repeated here. Suffice it to say that each is a function of the temperature, angular velocity and mass of the neutron star. Since $1/\tau_r$ is the imaginary part of the frequency of the *r*-mode, the mode is stable when $\tau_r > 0$ and unstable when $\tau_r < 0$. For a star of given temperature and mass, the critical angular velocity Ω_c is defined to be the angular velocity where $1/\tau_r = 0$. Stars rotating more rapidly than Ω_c are unstable while those rotating more slowly are stable.

We have evaluated the critical angular velocities Ω_c numerically using the new hyperon bulk viscosities derived in Sec. V. Figure 13 illustrates the temperature dependence of the critical angular velocities for a range of neutron-star masses. The more massive neutron stars have larger hyperon cores which suppress the *r*-mode instability more effectively. The curves in Fig. 13 assume that the Σ^- superfluid gap function is given by $\Delta_\Sigma = \Delta_\Lambda$, and that the axial vector coupling coefficients have their β-decay values. In Fig. 14 we compare the critical angular velocity curves for $1.4 M_\odot$ stellar models using either the $\Delta_\Sigma = \Delta_\Lambda$ (solid curve) or the $\Delta_\Sigma = 10\Delta_\Lambda$ (dash-dot curve) assumption about the Σ^- superfluid gap. The larger value of Δ_Σ allows superfluidity to make the bulk viscosity larger over a wider range of temperatures, and hence the *r*-mode instability is less effective. Also illustrated in Fig. 14 are the effects of changing various microphysics assumptions. The dotted curve shows the effect of changing the values of the axial vector coupling constants from their β-decay values to the asymptotic value -1. And the dashed curve shows the effect of using bare masses rather

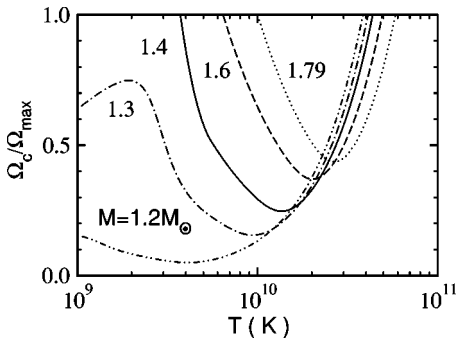

FIG. 13. Critical angular velocities for neutron stars as a function of hyperon core temperature. Each curve represents a neutron star of fixed mass, ranging from 1.2 $M_\odot$ to the maximum mass for this equation of state, 1.79 $M_\odot$. These curves assume $\Delta_\Sigma = \Delta_\Lambda$ and use the β-decay values of the weak axial vector coupling coefficients.

than the effective masses in the scattering cross sections. These alternative assumptions make the bulk viscosity less effective and the *r*-mode instability operates over a wider range of angular velocities in these stars. However, neither of these effects is as large as that resulting from a change in the superfluid gap.

The hyperons' primary contribution to the bulk viscosity of neutron-star matter is through the mechanism discussed above. However, as pointed out by Jones, the presence of hyperons in the core of a neutron star also makes it possible for alternate forms of the direct Urca interaction to take place and these too contribute to the bulk viscosity of the material. Jones showed that the contributions to the bulk viscosity from this process are given by

$$\mathrm{Re}\,\zeta = \frac{4.9\times 10^{30} T_{10}^{-4}}{1 + 2.0\times 10^{-6}\hat{\omega}^2 T_{10}^{-8}}, \tag{6.8}$$

in cgs units for typical values of neutron star matter, where T_{10} is the temperature measured in units of 10^{10} K. Using this expression in the Λ containing core of the neutron star, we have evaluated the effects of this hyperon channel direct

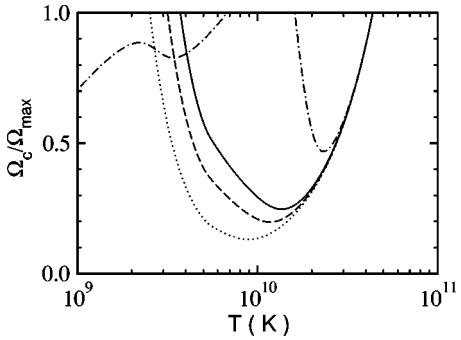

FIG. 14. Critical angular velocities for 1.4 $M_\odot$ neutron stars as a function of hyperon core temperature. The solid curve assumes that $\Delta_\Sigma = \Delta_\Lambda$ while the dot-dash curve assumes $\Delta_\Sigma = 10\Delta_\Lambda$. Both curves use the β-decay values of the weak axial vector coupling coefficients. Dotted curve uses $g_B = -1$, while dashed curve uses bare masses.

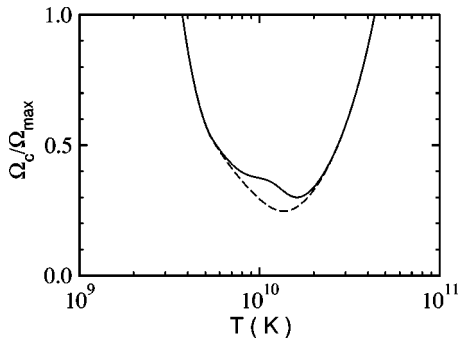

FIG. 15. Critical angular velocities for $1.4M_\odot$ neutron stars as a function of hyperon core temperature. Solid curve includes the effects of hyperon bulk viscosity, hyperon channel direct Urca bulk viscosity, and modified Urca bulk viscosity. Dashed curve leaves out the effects of the direct Urca hyperon bulk viscosity.

Urca bulk viscosity on the stability of the *r*-modes. These results are illustrated in Fig. 15. The solid curve in Fig. 15 includes the effects of the hyperon bulk viscosity discussed above, the hyperon channel direct Urca bulk viscosity of Eq. (6.8), and the ordinary modified Urca bulk viscosity. For comparison the dashed curve leaves out the effects of the hyperon channel direct Urca bulk viscosity. We see that this direct Urca bulk viscosity has only a small effect on the stability of the *r*-modes for temperatures around 10^{10} K.

VII. DISCUSSION

We have analyzed here the effects of the bulk viscosity due to hyperons on the stability of the *r*-modes in rotating neutron stars. Hyperons exist only in the high density core of a neutron star where the influence of the *r*-mode is quite small. Thus to evaluate accurately and reliably the importance of this effect, it was necessary to compute detailed and accurate models of the composition and structure of the neutron star core, and to have an accurate model of the structure of the *r*-mode in this region. We use Glendenning's [10,11] relativistic mean-field equation of state to evaluate the composition of the nuclear matter in the stellar core, and solve the relativistic Oppenheimer-Volkoff equations to determine the stellar structure.

Our evaluation of the hyperon bulk viscosity improves on previous work in several ways. First we generalize in Eqs. (3.11) and (3.14) the standard expression for the bulk viscosity coefficient so that it applies to relativistic fluids such as neutron star matter. Second we generalize the expressions in Eqs. (3.24) and (3.25) for the thermodynamic quantities that relate the microscopic reaction rates to the relaxation time that appears in the expression for the bulk viscosity by including fully interacting nuclear matter. And third we obtain in Eqs. (4.28) and (4.29) the fully relativistic expressions for the relevant hyperon scattering cross sections needed to evaluate the microscopic reaction rates. While our expressions for these cross sections reduce to the published low-momentum results, we find that the difference of Eq. (4.29) from the low-momentum limit can be an order of magnitude or more and reduces the coefficient of bulk viscosity somewhat at low densities. Finally we evaluate the effects of this hyperon bulk viscosity on the *r*-modes using an accurate model for the structure of the *r*-mode in the core of a neutron star.

Our results show that the hyperon bulk viscosity does not substantially suppress the gravitational radiation instability of the *r*-modes until the temperature of the core of the neutron star drops below a few times 10^9 K. [This is in spite of the fact that our coefficient of bulk viscosity is actually higher than that of Jones [2,3]. The expansion of the fluid in the core of the star as given in Eq. (6.6) is smaller than he estimated.] Below 10^9 K the *r*-mode instability is strongly suppressed in all of our models over the range of Σ^- superfluid gap functions and the range of axial vector coupling constants that we studied. If the core of the neutron star cools according to the standard modified Urca process [5], then it would remain hot enough for the *r*-mode instability to act for about a day. This is enough time for the *r*-mode to grow and radiate away through gravitational waves a substantial fraction of the rotational kinetic energy of a rapidly rotating neutron star [6]. However if the core of the neutron star cools substantially faster than this, then it may not be possible for the *r*-mode to grow rapidly enough to effect the star in a substantial way before the hyperon bulk viscosity stabilizes it. Cooling by the direct Urca process is significantly faster than the modified Urca process: cooling the core of a neutron star to a few times 10^9 K within about a second [7,8]. Cooling by the direct Urca process will occur in neutron-star matter whenever the proton/baryon ratio is larger than about 0.15. Since proton fractions in excess of this are now generally expected in neutron star matter, cooling by the direct Urca process seems likely at least until the temperature of the core falls below the superfluid transition temperature for neutrons or protons at about 10^9 K. Thus it appears likely that the *r*-mode instability is effectively suppressed by rapid cooling of the neutron star core and the non-leptonic hyperon bulk viscosity.

Once a neutron star cools below the transition temperature for the formation of neutron and proton superfluids, the relaxation time scale for the hyperon interactions will increase exponentially compared to the expressions derived here in Eqs. (5.1) and (5.2). This sharply reduces via Eq. (5.3) the bulk viscosity from this process at sufficiently low temperatures. Further detailed calculations would be needed to determine whether the hyperon bulk viscosity has a significant influence on the *r*-mode instability at temperatures of a few times 10^8 K, which are expected to exist in the cores of neutron stars in low-mass x-ray binaries. We did not carry out these calculations in part because solid crust-related shear [24,25] and magnetic field [26] effects are quite effective in suppressing the instability at these low temperatures.

How robust is the conclusion that the *r*-mode instability is effectively suppressed? Clearly the details of the nuclear physics involving hyperons in neutron star matter are not well understood at this time. However, our conclusion applies to the entire expected range of the most poorly known properties of this material: the superfluid Σ^- gap function and the axial vector coupling coefficients. In order to escape this conclusion, it would be necessary for neutron star matter to have very few hyperons present at the densities which

exist in the cores of real neutron stars. This would require the equation of state to be substantially different from the one studied here, or the masses of neutron stars to be significantly smaller than $1.4M_\odot$. Rapid rotation also lowers the central density and consequently the size of the hyperon core in a neutron star. The central density of a maximally rotating $1.4M_\odot$ neutron star is about 73% of its non-rotating value (for the equation of state studied here) [27]. This reduction almost eliminates the hyperon core for this extreme angular velocity, but over almost all of the range of angular velocities, $1.4M_\odot$ stars have substantial hyperon cores. Finally if the dissipation in the core were sufficiently large it might be possible for the *r*-mode eigenfunction to be clamped to zero in the core by the dissipative processes while remaining finite and unstable in the outer parts of the star. The discussion of this possibility in the Appendix shows that the hyperon bulk viscosity is not strong enough to clamp the *r*-mode in this way.

ACKNOWLEDGMENTS

We thank P. B. Jones for raising the issue of hyperon bulk viscosity, for communicating his unpublished work to us, and for giving us helpful comments on our work. We also thank S. Balberg, D. Chernoff, J. Friedman, N. Glendinning, P. Goldreich, J. Lattimer, G. Mendell, J. Miller, E. S. Phinney, M. Prakash, R. Sawyer, and K. Thorne for helpful discussions. This work was supported by NSF Grant Nos. PHY-9796079, PHY-0071028, PHY-0079683, and PHY-0099568, and NASA Grant Nos. NAG5-4093 and NAG5-10707.

APPENDIX: MODE CLAMPING

Bulk viscosity damps a mode by dissipating energy according to the expression

$$\frac{d\tilde{E}}{dt} = -\frac{\tilde{E}}{2\tau_B}. \tag{A1}$$

For the case of the *r*-modes in slowly rotating stars, we may express the energy, and its time derivative as simple radial integrals:

$$\tilde{E} = \int \epsilon dr, \tag{A2}$$

$$\frac{d\tilde{E}}{dt} = -\int \dot{\epsilon} dr, \tag{A3}$$

where ϵ and $\dot{\epsilon}$ are the angle averaged energy and energy dissipation rate densities respectively as given in Eqs. (6.4) and (6.5).

The mode will be completely suppressed (clamped) locally if the amount of energy removed from the mode locally in one oscillation period is comparable to the local energy density of the mode. Thus we define the local quality factor of the mode:

$$q = \frac{\hat{\omega}\epsilon}{2\pi\dot{\epsilon}}. \tag{A4}$$

If $q \lesssim 1$ the mode will be clamped. For the *r*-modes we find that

$$\frac{1}{q} \approx \frac{0.3\zeta}{\rho R^2 \Omega_{\max}} \left(\frac{r}{R}\right)^2 \frac{\Omega_{\max}}{\Omega}. \tag{A5}$$

For the $1.4M_\odot$ neutron star model considered here $\Omega_{\max} \approx 4700$ rad/s, $\rho \gtrsim 5\times 10^{14}$ g/cm^3 and $r \lesssim 6$ km in the region where hyperons occur, and $R \approx 14$ km. Thus

$$\frac{1}{q} \approx \frac{\zeta}{8\times 10^{31}} \frac{\Omega_{\max}}{\Omega} \tag{A6}$$

for this case. Figures 11 and 12 show that the bulk viscosity never exceeds about 10^{31} in the temperature range of interest to us. Thus, we conclude that the hyperon bulk viscosity represents a small perturbation on the basic hydrodynamic forces of the *r*-modes. The condition $q<1$ is violated only for relatively slowly rotating stars. In the domain where the gravitational radiation instability is most likely to be important, the dissipation by hyperons represents a small perturbation on the basic hydrodynamic forces, thus the *r*-modes will not be clamped.

[1] L. Lindblom, in *Gravitational Waves: A Challenge to Theoretical Astrophysics*, edited by V. Ferrari, J. C. Miller, and L. Rezzolla, ICTP Lecture Notes Series, Vol. 3 (ICTP, Triest, 2001).
[2] P. B. Jones, Phys. Rev. Lett. **86**, 1384 (2001).
[3] P. B. Jones, Phys. Rev. D **64**, 084003 (2001).
[4] P. B. Jones, Proc. R. Soc. London, Ser. A **323**, 111 (1971).
[5] S. L. Shapiro and S. A. Teukolsky, *Black Holes, White Dwarfs, and Neutron Stars* (Wiley, New York, 1983).
[6] L. Lindblom, J. E. Tohline, and M. Vallisneri, Phys. Rev. Lett. **86**, 1152 (2001).
[7] C. J. Pethick and V. Thorsson, in *Lives of the Neutron Stars*, edited by A. Alpar, Ü. Kiziloglu, and J. van Paradijs (Kluwer, Dordrecht, 1995).
[8] D. Page, M. Prakash, J. M. Lattimer, and A. Steiner, Phys. Rev. Lett. **85**, 2048 (2000).
[9] L. Lindblom, B. J. Owen, and S. M. Morsink, Phys. Rev. Lett. **80**, 4843 (1998).
[10] N. K. Glendenning, Astrophys. J. **293**, 470 (1985).
[11] N. K. Glendinning, *Compact Stars*, 2nd ed. (Springer, New York, 2000).
[12] L. D. Landau and E. M. Lifshitz, *Fluid Mechanics*, 2nd ed. (Butterworth-Heinemann, Oxford, 1999).
[13] S. Balberg and N. Barnea, Phys. Rev. C **57**, 409 (1998).
[14] T. Takatsuka, S. Nishizaki, Y. Yamamoto, and R. Tamagaki, Prog. Theor. Phys. **105**, 179 (2001).
[15] B. Mühlschlegel, Z. Phys. **155**, 313 (1959).
[16] D. J. Griffiths, *Introduction to Elementary Particles* (Wiley, New York, 1987).

[17] Particle Data Group, D. E. Groom *et al.*, Eur. Phys. J. C **15**, 1 (2000). See also http://pdg.lbl.gov/

[18] G. W. Carter and M. Prakash, nucl-th/0106029.

[19] P. Haensel, K. P. Levenfish, and D. G. Yakovlev, astro-ph/0110575, appeared on the Los Alamos archive shortly after we submitted this paper. Haensel *et al.* perform a hyperon bulk viscosity calculation analogous to ours for the case of the Σ^- reaction (4.1) only, but they obtain a coefficient of bulk viscosity ζ ten times greater than ours. Most of this factor $(5+)$ is due to their taking the limiting value (4.10) for $|\mathcal{M}_\Sigma|^2$, which is anomalously small. The critical angular velocity for the *r*-mode instability scales as $\zeta^{1/6}$, and thus Haensel *et al.* would obtain critical angular velocities about $10^{1/6}=1.5$ times the values we obtain in Sec. VI.

[20] D. Pines and P. Nozières, *The Theory of Quantum Liquids* (Benjamin, New York, 1966), Vol. I.

[21] L. Lindblom, G. Mendell, and B. J. Owen, Phys. Rev. D **60**, 064006 (1999).

[22] N. Andersson, Astrophys. J. **502**, 708 (1998).

[23] J. L. Friedman and S. M. Morsink, Astrophys. J. **502**, 714 (1998).

[24] L. Bildsten and G. Ushomirsky, Astrophys. J. Lett. **529**, L33 (2000).

[25] L. Lindblom, B. J. Owen, and G. Ushomirsky, Phys. Rev. D **62**, 084030 (2000).

[26] G. Mendell, Phys. Rev. D **64**, 044009 (2001).

[27] We use a modified version of N. Stergioulas' *RNS* code to compute the structures of the rotating relativistic stellar models, http://gravity.phys.uwm.edu/rns/